Proceedings of the
International Conference on Mechanical Engineering 2011
(ICME2011) 18-20 December 2011, Dhaka, Bangladesh

ICME11-RT-021

EFFECT OF SINTERING TEMPERATURE ON THE STRUCTURAL AND ELECTROMAGNETIC PROPERTIES OF NiCuZn FERRITE

M. Belal Hossen[1], N. A. Ahmad[2] and A. K. M. Akther Hossain[3]

[1] Department of Physics, Chittagong University of Engineering and Technology, Bangladesh
[2] Industrial Physics Division, BCSIR Laboratory, Dhaka, Bangladesh
[3] Department of Physics, Bangladesh University of Engineering and Technology, Bangladesh.

ABSTRACT

The effect of sintering temperature (T_S) on the structural and electromagnetic properties of NiCuZn ferrite of chemical formula $Ni_{0.27}Cu_{0.10}Zn_{0.63}Fe_2O_4$ which prepared by standard double sintering ceramic technique has been studied. Samples were sintered at various T_s (1373, 1423, 1473, 1523 and 1573K) for 5h in air. X-ray diffraction (XRD) patterns indicated the presence of a single phase spinel structure. The bulk densities (ρ_B) are correlated with T_s. Scanning Electron Microscopy (SEM) showed that the average grain size (D) increased with increasing T_s. The complex initial permeability spectra and relative quality factor (Q) significantly changed with T_s. The high permeability at various T_S was due to increase grain size, better densification, lower magnetostriction constant and inner stresses etc. The temperature dependence real part of initial permeability was measured, on toroidal shaped samples at constant frequency of 100 kHz and Néel temperature (T_N) was determined. It was found that at various T_S, the complex initial permeability with no considerable effect for it on the value of T_N. The dielectric constant (έ) of all the samples showed a significant relation with sintering temperature and decrease with increase in frequency exhibiting normal ferrimagnetic behavior. The variation of dielectric loss tangent with frequency showed maxima in the 0.45-4300 kHz frequency range. These maxima are also found to shift towards high frequency region as the T_s increases. All the variations are explained on the basis of Cu^{2+} and Cu^{+}; Ni^{2+} and Ni^{3+}; Fe^{2+} and Fe^{3+} concentrations on octahedral sites and electronic hopping frequency between Fe^{2+} and Fe^{3+} ions and hole transfer between Cu^{2+} and Cu^{+}; Ni^{2+} and Ni^{3+} over octahedral site. A possible correlation and explanations for observed structural and electromagnetic properties of $Ni_{0.27}Cu_{0.10}Zn_{0.63}Fe_2O_4$ at various T_S are given on the basis of existing theory.

Keywords: NiCuZn Ferrite, Sintering Temperature, Initial Permeability and Dielectric Loss.

1. INTRODUCTION

Various super lightweight equipments including mobile phones, portable computer, liquid crystal display and plasma display panel, need miniature DC–DC converters, inductors for filter and signal amplifying power inductors in circuit. Thus, it is necessary to realize miniaturization of electromagnetic components. Compared with MnZn ferrites that are already widely used in the miniature DC–DC converters and inductors [1-2]. The NiCuZn spinel ferrites are soft magnetic materials, which have wide application in advanced technologies such as multilayer chip inductors [3], multilayer LC filters [4], magnetic temperature sensors [5] and humidity sensors [6]. Several investigations have focused their attention on NiCuZn spinel ferrites because copper containing ferrites have interesting electrical and magnetic properties. Copper ferrite is distinguished among other spinel ferrites by the fact that it undergoes a structural phase transition accompanied by a reduction in the crystal symmetry to the tetrahedral due to the Cooperative Jahn–Teller effect [7]. Various methods have been developed to fabricate NiCuZn ferrites. The crystal structure and particle size of the materials control their physical as well as electromagnetic properties, which depend entirely on the method of preparation, nature and concentration of dopant [8-9]. In this research we are interested to investigate the effect of various T_s on structural and electromagnetic properties of $Ni_{0.27}Cu_{0.10}Zn_{0.63}Fe_2O_4$.

2. EXPERIMENTAL

The $Ni_{0.27}Cu_{0.10}Zn_{0.63}Fe_2O_4$ sample was prepared using the standard double sintering ceramic technique. Powders of NiO (99.9%), CuO (99.9%), ZnO (99.9%) and Fe_2O_3 (99.9%) were used as raw materials. Stoichiometric amounts of required powders were mixed thoroughly and then calcined at 1173K for 5h. The calcined powders were then pressed into disk and toroid-shaped samples. The samples were sintered at 1373, 1423, 1473, 1523 and 1573K for 5h in air. The temperature ramp for sintering was 10K/min for heating, and 5K/min for cooling. The structural characterization was carried out with an X-ray diffractometer CuKα radiation. The lattice parameter for the composition was

calculated using Nelson–Riley function [10]. The theoretical density, (ρ_{th}), was calculated using the relation, $\rho_{th} = (8M_A)/(N_A a^3)$, where N_A is Avogadro's number, M_A is the molecular weight of the composition and 'a' is the lattice constant. The porosity (P) was calculated using the formula $P(\%) = ((\rho_{th} - \rho_B)/ \rho_{th})100$, where ρ_B (mass/volume) is the bulk density. Surface morphology and microstructure of the samples were studied with a SEM. Average grain sizes (grain diameter) of the sample were determined from SEM micrographs by linear intercept technique [11]. The frequency characteristics of $Ni_{0.27}Cu_{0.1}Zn_{0.63}Fe_2O_4$ ferrite sample i.e. the initial permeability spectra were investigated using a Wayne Kerr Precision Impedance Analyzer (model no. 6500B). The complex initial permeability measurements on toroid shaped samples have been carried out at room temperature of the sample in the frequency range 100Hz-120MHz. The values of the measured parameters obtained as a function of frequency and the real part (μ_i') of the complex initial permeability have been calculated using the following relations: $\mu_i' = L_s/L_0$, where L_s is the self inductance of the sample core and $L_0 = (\mu_0 N^2 h/2\pi)\ln(r_0/r_i)$ is derived geometrically, where L_0 is the inductance of the winding coil without the sample core, N is the number of turns of the coil (N=3), h is the thickness, r_0 is the outer radius and r_i is the inner radius of the toroidal specimen. The Q factor was calculated from the relation: $Q = \mu_i'/\tan\delta$, where tanδ is the loss factor. The temperature dependent permeability was measured at a fixed frequency (100 kHz). The T_N was calculated from the temperature-dependent permeability measurement. The έ and dielectric loss tangent were measured in the frequency range 100Hz-120MHz at room temperature using the above mentioned impedance analyzer by two probe method.

3. RESULTS AND DISCUSSION

3.1 Structural and Surface Morphology

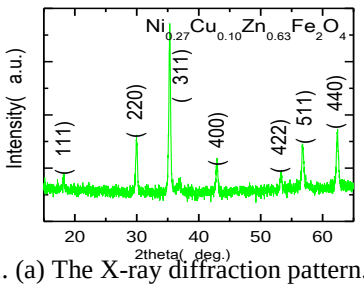

Fig 1. (a) The X-ray diffraction pattern. (b) The Nelson-Riley function F(θ) vs lattice parameter for $Ni_{0.27}Cu_{0.10}Zn_{0.63}Fe_2O_4$.

Table 1: The lattice constant, density, porosity, grain size, natural resonance frequency, maximum Quality factor and initial permeability of the various $Ni_{0.27}Cu_{0.10}Zn_{0.63}Fe_2O_4$ ferrites sintered at various temperatures, T_s, for 5 h in air.

T_s (K)	a_o (nm)	$\rho_{x\text{-ray}}$ 10^3 (kg/m^3)	ρ_B*10^3 (kg/m^3)	P (%)	Grain size (μm)	f_r (MHz)	Q_{max}	μ_i' (at 1.01 kHz)
1373	0.841	5.32	3.97	25.2	1.45	18.1	2418	182
1423			4.72	11.2	2.57	6.55	5912	754
1473			4.76	10.4	207	2.25	5881	1353
1523			4.67	12.1	398	1.92	7000	1524
1573			4.11	22.6	417	0.71	9938	1684

The XRD pattern for $Ni_{0.27}Cu_{0.10}Zn_{0.63}Fe_2O_4$ sample is shown in Fig 1(a). The XRD pattern clearly shows the single phase and formation of spinel structure. Analyzing the XRD patterns authors detect that the positions of the peaks comply with the earlier reported value [12]. The values of lattice parameter of all the peaks for the sample is plotted against Nelson-Riley function, F(θ), in Fig 1(b). Fig 2 shows the ρ_B and P as a function of T_s. The ρ_B of the $Ni_{0.27}Cu_{0.10}Zn_{0.63}Fe_2O_4$ sample increases as the T_s increases from 1373 to 1473K and above 1473K the density decreases gradually. On the other hand, P of the samples decreases, as increasing T_s up to 1473K, and above 1473K the P increases. The increase in ρ_B with

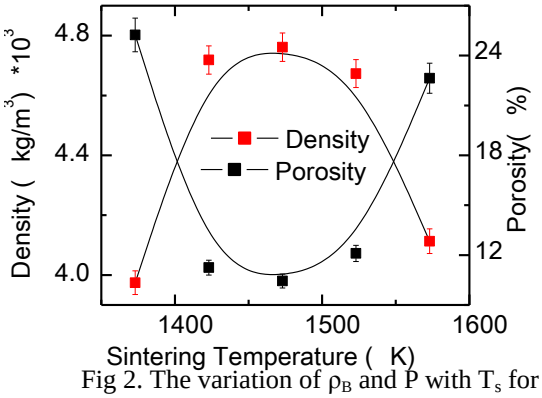

Fig 2. The variation of ρ_B and P with T_s for $Ni_{0.27}Cu_{0.10}Zn_{0.63}Fe_2O_4$.

T_s is expected. This is because during the sintering process, the thermal energy generates a force that drives the grain boundaries to grow over pores, thereby decreasing the pore volume and denser the material. At higher T_s's the ρ_B decreases because the intragranular P increases resulting from exaggerated grain growth which is shown in Fig 3. When the grain growth rate is very high, pores may be left behind by rapidly moving grain boundaries, resulting in pores that are trapped inside the grains.

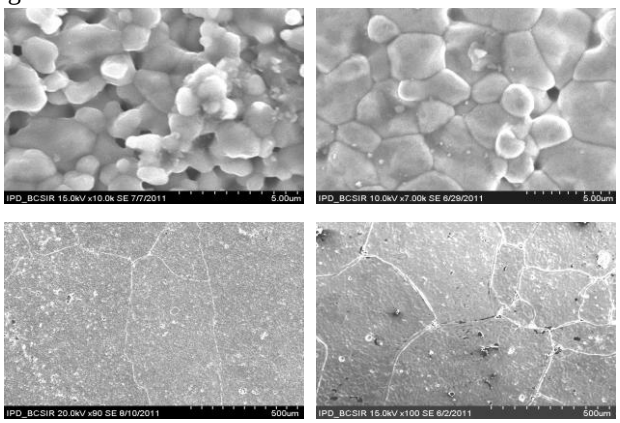

Fig 3. The SEM micrographs of $Ni_{0.27}Cu_{0.10}Zn_{0.63}Fe_2O_4$ sample sintered at (a) 1373K, (b) 1423K, (c) 1523K, (d) 1573K.

The discontinuous growth of grain rises with temperature and hence, contributing toward the reduction of the bulk density. Such a conclusion is in agreement with that previously reported in case of NiMnZn ferrites [13].
The typical SEM micrographs of $Ni_{0.27}Cu_{0.10}Zn_{0.63}Fe_2O_4$

sintered at various T_s are shown in Fig 3. The grain size is significantly increases with T_s. The average D increases from 1.45 to 417 μm with increasing sintering temperature up to 1573K. The uniformity in the grain size and the average D can control materials properties such as the magnetic permeability. The behavior of grain growth reflects the competition between the driving force for grain boundary movement and the retarding force exerted by pores [14]. When the driving force of the grain boundary in each grain is homogeneous, the sintered body attains a uniform grain size distribution; in contrast, discontinuous grain growth occurs if this driving force is inhomogeneous.

3.2 Initial Permeability and Néel Temperature

Figure 4 shows the complex initial permeability spectra for $Ni_{0.27}Cu_{0.10}Zn_{0.63}Fe_2O_4$ sample sintered at 1373, 1423, 1473, 1523 and 1573K. It is observed that the μ_i' of $Ni_{0.27}Cu_{0.10}Zn_{0.63}Fe_2O_4$ increases from 182 to 1684 as T_s increases from 1373 to 1573K. The variation of μ_i' with frequency for the composition can be explained on the basis of Globus model. According to this model, the relaxation character is $(\mu_i'-1)^{1/2}f_r$ = constant, where f_r is the natural resonance frequency [15].The μ_i' of ferrite is related by $\mu_i' \approx M_s^2 D/\sqrt{K_1}$, where M_s is the saturation magnetization, K_1 is the magnetocrystalline anisotropy constant and D is the average grain diameter [15]. The increase in μ_i' with increasing T_s can be attributed to the increase in D, which increases with increasing Ts, as shown in Fig 3. Increase in D results in an increase in the number of domain walls in each grain. As the movement of walls determines the μ_i', an increase in number of domain walls would result in an increase in μ_i'. Thus for a large grain the μ_i' should increase as it varies proportionally with D. So we can expect higher μ_i' for the samples sintered at higher T_s. Though above 1473K, ρ_B decreases i.e. increase the number of pores within the grain but grain size increases which results increase in μ_i'. The pores act as pinning sites for the domain wall movement. Consequently, domain wall movement is restricted and this limits the rate of growth of μ_i'. It is also observed that f_r decreases with increase in T_s. As T_s increases, the f_r shifted from 18.1 to 0.71 MHz. Since the relaxation frequency of domain wall oscillation is inversely proportional to D [16], so f_r observed in the present work is expected to shift toward lower frequency with the increase in T_s. Fig 4(b).shows μ_i'' as a function of frequency and it is observed that μ_i'' increase with the increase of T_s. At lower frequencies, the lag of domain wall motion with respect to the applied magnetic field is responsible for magnetic loss and at higher frequencies, a rapid increase in loss factor is observed. A resonance loss peak is shown in this rapid increase of magnetic loss. At resonance, maximum energy transfer occurs from the applied field to the lattice which results the rapid increases in loss factor. Fig 5 shows the variation of Q with frequency for $Ni_{0.27}Cu_{0.10}Zn_{0.63}Fe_2O_4$ sintered at various T_s. The maximum Q value (Q_{max}) gradually increases with increasing T_s in the range 2418-9938 except at T_s=1473K which is slightly smaller than that of T_s=1423K. Initially the value of Q_{max} frequency decreases with the increase of T_s but at higher T_s there is no significant change in Q_{max} value frequency. At higher frequencies, Q decreases rapidly. The rapid decrease shows the tendency for a resonance loss peak. The Q value depends on the ferrites microstructure, e.g. pores and grain size etc.

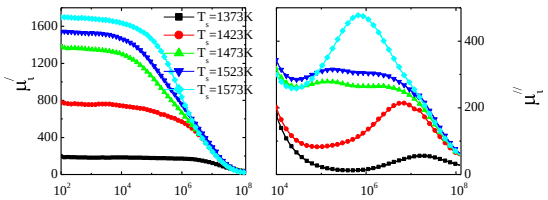

Fig 4. shows the complex initial permeability spectra, (a) μ_i' and (b) μ_i'' for $Ni_{0.27}Cu_{0.10}Zn_{0.63}Fe_2O_4$ sample sintered at 1373, 1423, 1473, 1523 and 1573K.

Fig 6 shows μ_i' as a function of temperature for $Ni_{0.27}Cu_{0.10}Zn_{0.63}Fe_2O_4$ sintered at various T_s. The T_N is determined from temperature dependent permeability measurement which is 383K. The T_N, is a function of the magnitude of the exchange energy.

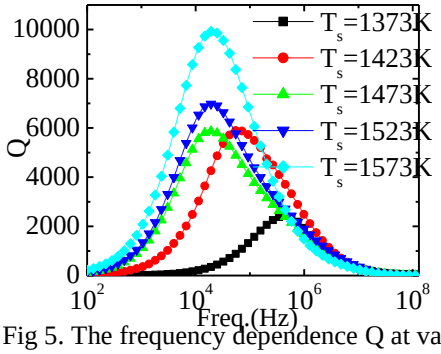

Fig 5. The frequency dependence Q at various T_s.

Physically, at T_N, the thermal agitation is so high that it reduces the alignment of the magnetic moment along a given axis to zero [15]. It follows that a ferrimagnetic material above its T_N is paramagnetic. Furthermore, it has been shown that the sharpness of the permeability drops at the T_N can be used as a measure of the degree of compositional homogeneity. The $Ni_{0.27}Cu_{0.10}Zn_{0.63}Fe_2O_4$ shows good homogeneity.

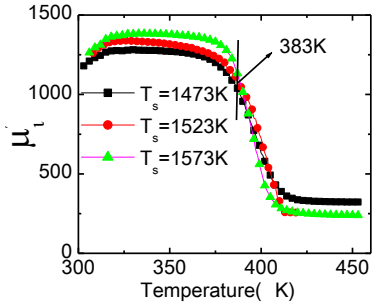

Fig 6. The temperature dependence of real part of initial permeability at various T_s.

3.3 Frequency Dependence of Dielectric Constant

Figure 7(a) shows the variation of dielectric constant with frequency in the range 100 Hz-120 MHz. The variation of έ with frequency reveals the dispersion due to Maxwell-Wagner [17] type interfacial polarization in agreement with Koops phenomenological theory [18]. The έ decreases with increasing frequency reaching a constant value for all the samples.

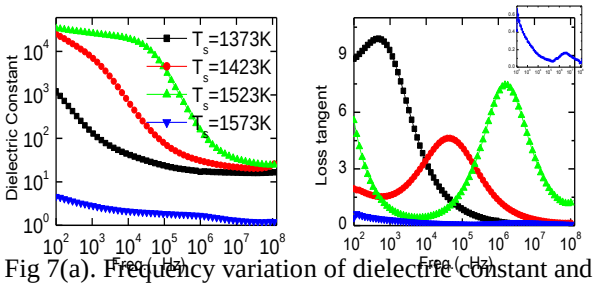

Fig 7(a). Frequency variation of dielectric constant and loss tangent of various T_s at room temperature.

According to Iwauchi [19], the polarization in ferrites is through a mechanism similar to the conduction process. By electron exchange between $Fe^{2+} \Leftrightarrow Fe^{3+}$, one obtains local displacement of electrons in the direction of the applied field and these electrons determine the polarization. It was [20] suggested that, for copper and nickel containing ferrite, Cu^{2+} and Ni^{3+} ions can be formed during the sintering process due to reduction tendency of $Cu^{2+} \Leftrightarrow Cu^{+}$ and $Ni^{2+} \Leftrightarrow Ni^{3+}$. It is known that, in the case of zinc containing ferrite a partial reduction of Fe^{3+} ions to Fe^{2+} ion can take place as a result of volatilization of zinc during the sintering process [20]. It was also suggested that, the presence of Cu^{2+} and Ni^{2+} on the octahedral site fervors the following exchange interaction [21]:

$$Ni^{2+} + Fe^{3+} \Leftrightarrow Ni^{3+} + Fe^{2+}$$

Or

$$Ni^{2+} + Cu^{2+} \Leftrightarrow Ni^{3+} + Cu^{+}$$

Thus the conduction mechanism for the samples under investigation can be explain by two exchange interactions: electron hopping between Fe^{2+} and Fe^{3+} and hole transfer between Cu^{2+} and Cu^{+}; Ni^{3+} and Ni^{2+} over the octahedral sites. The first exchange give rise to the displacement of the local charges in the direction of the external field leading to the main source of polarization in these ferrites, while the latter exchange gives rise to displacement of the holes in opposite direction of the external field leading to the second source of polarization in these ferrites. The decrease of the έ with increasing frequency can be attributed to the fact that the electron exchange interaction between ferrous and ferric ions and hole exchange between Cu^{2+} and Cu^{+}; Ni^{3+} and Ni^{2+} cannot follow the frequency of the external alternating electric field beyond a certain frequency value [21]. The large values of έ at lower frequencies are due to the predominance of the species like Fe^{2+} ions, interfacial dislocation pile ups, oxygen vacancies, grain boundary defects, etc. [17]. While the decrease in έ with frequency is natural because of the fact that any species contributing to polarisability is bound to show lagging behind the applied field at higher and higher frequencies. Koops [18] gave the phenomenological theory for the dielectric dispersion in ferrites at low frequencies. Koops was among the first to study the frequency dependence of dielectric constant and dispersion of ferrites. He interpreted the result by considering the dielectric as an inhomogeneous medium of a Maxwell-Wagner type. In the present system the dispersion in έ with frequency can be attributed to be caused by Maxwell-Wagner type interfacial polarization.

3.4 Frequency Variation of Loss Tangent

The variation of loss tangent with frequency is shown in the Figs 7(b). All the samples show dispersion in tanδ, which can be explained from the following relation [22]:

$$\text{Tan}\delta = 1/(\omega \acute{\varepsilon} \varepsilon_0 \rho') \qquad (1)$$

where ω is the angular frequency corresponding to maximum value of tanδ. A maximum value of tanδ is observed when the jump frequency of electron between Fe^{2+} and Fe^{3+} is equal to the frequency of the applied field [23]. From the plots of tanδ versus frequency, it can be seen that the curves for samples with various [T_s=1373, 1423, 1523, 1573K] T_s show maxima at frequencies ranging from 451Hz to 4.3MHz. The sample with T_s=1573K show smaller such maxima which shows inset of Fig 6(b). It is interesting to know that f_{max} shifts towards higher frequency side with increasing T_s.
The shifting of f_{max} towards high-frequency side can be explained as follows.

It is an established fact that the condition for observing a maximum in the dielectric loss of a dielectric material is given by the relation

$$\omega\tau = 1 \qquad (2)$$

where $\omega = 2\pi f_{max}$ and τ is the relaxation time. Now, the relaxation time τ is related to the jumping probability per unit time 'P' by an equation

$$\tau = 1/2P$$

or

$$f_{max} = (1/\pi)P \qquad (3)$$

Eq. (3) shows that f_{max} is proportional to hopping probability. Now a continuous increase of f_{max} with increasing T_s indicates that hopping probability per unit time is increasing continuously. Since the direction of displacement of electrons is opposite to that of holes under the application of external field, the mobility of holes is relatively very small with respect to that of electrons. The resultant polarization of both types of charge carriers will give peaking behavior as shown in Fig 6(b). The shift of the peak to higher frequency with increasing temperature may be attributed to the corresponding increase of the mobility of the charge carriers with temperature. A qualitative explanation can be given for the occurrence of the maxima in the tanδ versus frequency curves. As pointed out by Iwauchi [19], there is a strong correlation between the conduction mechanism and dielectric behaviour of the ferrites. The conduction mechanism in n-type ferrites is considered as due to hopping of electrons between Fe^{2+} and Fe^{3+} situated on the octahedral sites. As such when the hopping frequency is nearly equal to that of externally applied field a maximum of loss tangent may be observed [19]. Thus, it is possible that for the samples

with various T_s the hopping frequencies are of the appropriate magnitude to observe a loss maximum are 0.45, 42.9, 1610 and 4300kHz, respectively.

4. CONCLUSION

Phase pure $Ni_{0.27}Cu_{0.10}Zn_{0.63}Fe_2O_4$ is prepared by the standard double sintering ceramic technique. The XRD pattern confirms that the sample exhibit cubic spinel structure. The μ_i' and microstructure are strongly depend on T_s. Thus it can be concluded that to improve μ_i' by microstructural variation, the ferrites must be sintered at optimum temperature. Although pore and grain boundary would obstruct the movement of domain wall. The T_N is independent on T_s. The values of the dielectric constant at relatively low frequencies were very high and were attributed to the existence of interfacial polarization arising due to the inhomogeneous structure of the ferrite materials. Dielectric relaxation peaks on tanδ with frequency curves were observed and explained on the basis of the assumption that the mechanism of the dielectric polarization is similar to that of the conduction mechanism in these ferrites.

5. REFERENCES

1. Qi, X., Zhou, J., Yue, Z., Gui, Z., Li, L., 2002, "Effect of Mn substitution on the magnetic properties of MgCuZn ferrites", J. Magn. Magn. Mater. 251: 316-322.
2. Sun, K., Lan, Z., Yu, Z., Jiang, X., Huang, J., 2011, "Phase formation, grain growth and magnetic properties of NiCuZn ferrites", J. Magn. Magn. Mater. 323:927–932
3. Su, H., Zhang, H.W., Tang, X.L., Jia, L.J., Wen, Q.Y., 2006, "Sintering characteristics and magnetic properties of NiCuZn ferrites for MLCI applications", Mater. Sci. Eng. B 129:172–175.
4. Miao, C.L., Zhou, J., Cui, X.M., Wang, X.H., Yue, Z.X., Li, L.T., 2006 "Cofiring behavior and interfacial structure of NiCuZn ferrite/PMN ferroelectrics composites for multilayer LC filters", Mater. Sci. Eng. B 127:1–5.
5. Miclea, C., Tanasoiu, C., Miclea, C.F., Gheorghiu, A., Tanasiou, V., 2005, "Soft ferrite materials for magnetic temperature transducers and applications", J. Magn. Magn. Mater. 290–291:1506–1509.
6. Rezlescu, N., Doroftei, C., Popa, P.D., 2007, "Humidity sensitive electrical resistivity of $MgFe_2O_4$ and $Mg_{0.9}Sn_{0.1}Fe_2O_4$ porous ceramics", Rom. J. Phys. 52 3–4:353–360.
7. Manjura Hoque, S., Amanullah Choudhury, Md., Fakhrul Islam, Md., 2002, "Characterization of Ni–Cu mixed spinel ferrite", J. Magn. Magn. Mater. 251:292–303.
8. Hankare, P.P., Kamble, P.D., Kadam, M.R., Rane, K.S., Vasambeker, P.N., 2007, "Effect of sintering temperature on the properties of Cu–Co ferrites prepared by oxalate precipitation method", Mater. Lett. 61:2769–2771.
9. Hemeda, O.M., 2004, "Structural and Magnetic properties of $Co_{0.6}Zn_{0.4}Mn_xFe_{2-x}O_4$", Turk. J. Phys. 28:121–132.
10. Nelson, J.B., Riley, D.P., 1944, "An experimental investigation of extrapolation methods in the derivation of accurate unit-cell dimensions of crystals", Cavendish Laboratory, Cambridge.
11. Hossain, A. K. M., 1998, "Investigation of colossal magnetoresistance in bulk and thick film magnetites", Ph. D. Thesis, Imperial College, London.
12. Hossain, A. K. M., Kabir, K. K., Seki, M., Kawai, T., Tabata, H., 2007, "Structural, AC, and DC magnetic properties of $_{Zn1-x}Co_xFe_2O_4$", J. Phys. Chem. Solids. 68:1933-1939.
13. Hossain, A. K. M., Biswas, T. S., Mahmud, S. T., Yanagida, T., Tanaka, H., Kawai, T., 2009, "Enhancement of initial permeability due to Mn substitution in polycrystalline $Ni_{0.50-x}$ Mn_x $Zn_{0.50}$ Fe_2O_4" J. Magn. Magn. Mater. 321:81-87.
14. Costa, A. C. F. M., Tortella, E., Morelli, M. R., Kiminami, R. H. G. A., 2003, "Synthesis, microstructure and magnetic properties of Ni–Zn ferrites", J. Magn. Magn. Mater. 256:174-182.
15. Chauhan, B. S., Kumar, R., Jadhavc, K. M., Singh, M., 2004, "Magnetic study of substituted Mg–Mn ferrites synthesized by citrate precursor method", J. Magn. Magn. Mater. 283:71-81.
16. Goldman, A., 1999, *"Handbook of Modern Ferromagnetic Materials"*, Kluwer Acad. Pub, Boston, U.S.A.
17. [Maxwell, J.C., 1973, *"Electricity and Magnetism"*, 1:828, Oxford Univ. Press, New York.
18. Koops, C. G., 1951, "On the Dispersion of Resistivity and Dielectric Constant of Some Semiconductors at Audio frequencies", Phys. Rev. 83:121–124.
19. Iwauchi, K., 1971, "Dielectric Properties of Fine Particles of Fe_3O_4 and Some Ferrites", Jap. J. Appl. Phys. 10:1520-1528.
20. Zaki, H.M., "AC conductivity and frequency dependence of the dielectric properties for copper doped magnetite", 2005, Phy. B 363:232-244.
21. Tang, X. X., Manthiram, A., Goodenough, J. B., 1989 "Copper Ferrite Revisited," *.J Sol. Sta. Chem.* **79**:250-262.
22. Shaikh, A.M., Bellad, S.S., Chougule, B.K., 1999, "Temperature and frequency-dependent dielectric properties of Zn substituted Li-Mg ferrites", 195:384-390.
23. Reddy, M. B., Reddy, P. V., 1991, "Low-frequency dielectric behaviour of mixed Li-Ti ferrites", J. Phys. D: Appl. Phys. *24:975*

6. NOMENCLATURE

Symbol	Meaning	Unit
ρ_{th}	Theoretical density	(kg/m^3)
ρ_B	Bulk density	(kg/m^3)
μ_i'	Real part of initial permeability	Dimensionless
a	Lattice parameter	(nm)
P	Porosity	Dimensionless
Q	Relative quality factor	Dimensionless
T_N	Néel temperature	(K)
έ	dielectric constant	Dimensionless

7. MAILING ADDRESS

M. Belal Hossen
Department of Physics,
Chittagong University of Engineering and Technology,
Bangladesh